



iJRASET

International Journal For Research in
Applied Science and Engineering Technology



INTERNATIONAL JOURNAL FOR RESEARCH

IN APPLIED SCIENCE & ENGINEERING TECHNOLOGY

Volume: 10 **Issue:** III **Month of publication:** March 2022

DOI: <https://doi.org/10.22214/ijraset.2022.41015>

www.ijraset.com

Call: ☎ 08813907089

E-mail ID: ijraset@gmail.com

Application of Sentinel-2 Data for Extraction of Flood Inundation along Ganga River, Bihar

Manisha Kashyap¹, Chandra Mohan Bhatt², J. S. Rawat³

¹ Remote Sensing and GIS Department, Kumaun University, SSJ Campus, Almora, India

² Disaster Management Sciences Department, IIRS (ISRO), Dehradun, India

³ Department of Geography, Kumaun University, SSJ Campus, Almora, India

Abstract: Remote Sensing techniques played a significant role in the extraction of the flood inundation. The study is based on delineating the flood water of 2019 that affected the Bihar region along the Ganga River using Sentinel 2 satellite imageries. For this purpose the spectral water index methods: NDWI and MNDWI was used. And to differentiate water from the non-water areas certain threshold values were used. The selection of optimum threshold values was an essential task as it helped to precisely detect the inundated areas. The optimum threshold was lower for MNDWIs for the pre-flood time while for the during flood time NDWI the values were lower. For the pre-flood moment NDWI gave the highest Kappa of 0.93 and for the during flood moment, MNDWI 1 produced the highest Kappa of 0.95 and Overall Accuracy (OA) of 0.91. Overall in this experiment, MNDWI 1 estimated better accuracy in determining the water bodies and flooded region. Due to the highest rainfall in the districts of Patna, Khagaria, Begusrai, and Bhagalpur throughout, the areas were adversely affected by floods in 2019.

Keywords: Water Index, NDWI, MNDWI, Flood Inundation, Sentinel-2, natural disasters, Accuracy Assessment

I. INTRODUCTION

Flood takes place when a land which is usually dry gets covered with water, this might happen in a number of ways (National Geographic Floods). The most rapid floods takes place in rivers and it is the pricey disaster affecting large number of countries (Zwenzner, H., et al. 2009). Flooding leads to a considerable amount of social and economic damages (DMSG, 2001). With the innovation of Remote Sensing and GIS we can map and monitor flood with the associated data provided by the satellites (Rastogi, A.K, et al. 2018). The flood maps are useful for planning purposes, helps in making disaster mitigation plans, understand the overflow rate (Goodell, C., et al. 2006). GIS has a vital role to delineate the disaster area and overcome the flood issues (Rai, Praveen Kumar, et al. 2014). The Normalized Difference Water Index (NDWI) helps to maximize the water reflection when Green wavelength of the electromagnetic spectrum is minimized by NIR and water feature (Xu, et al. 2006). The multispectral imageries from Sentinel – 2 with its high spatial and temporal resolution provide free access to gather considerable data that can be used to map the water in the region (Du Yun et.al 2016). The Modified Normalized Difference Index (MNDWI) is significant in delineating flood water areas. The difference in the moist soil from non – water and water can be made through the reflectance of the two features (Ho L. T. K., et al. 2010).

II. SUDY SITE & DATASET

A. Site

The study site for this particular work is located in the Central Bihar along the River Ganga which is extended from 25°N to 26° N latitude and 85° E to 87° E longitude (**Figure 1**). The River Ganga which flow from west to east through the middle of the Bihar plain divides the state two unequal halves (North Bihar and South Bihar). The Ganges flows west to east and often floods most of the part of Bihar plain. The Mahananda, Gandak, Kosi, Bagmati, Kamala, Balan, Budhi Gandak are the major rivers of North Bihar. The rivers: Gandak and Koshi originate from the Nepal Himalayas while from the Kathmandu Valley originates the Bagmati. One of the most flood affected region of India is Bihar. The geographical and topographical location of the state makes it the most prone area to be affected by flood. The River Ganga passing the state causes flood every year which leads to large amount of loss to the economy of the state as well the flora and fauna of the region. Among the whole Bihar state, more than half of the population lives in the vulnerable parts. Each year the disaster causes large number of deaths of people which is again a major concern of the region. The destruction of human lives along with the assets makes massive loss. The research area covers the major flood affected zone of the state during 2019.

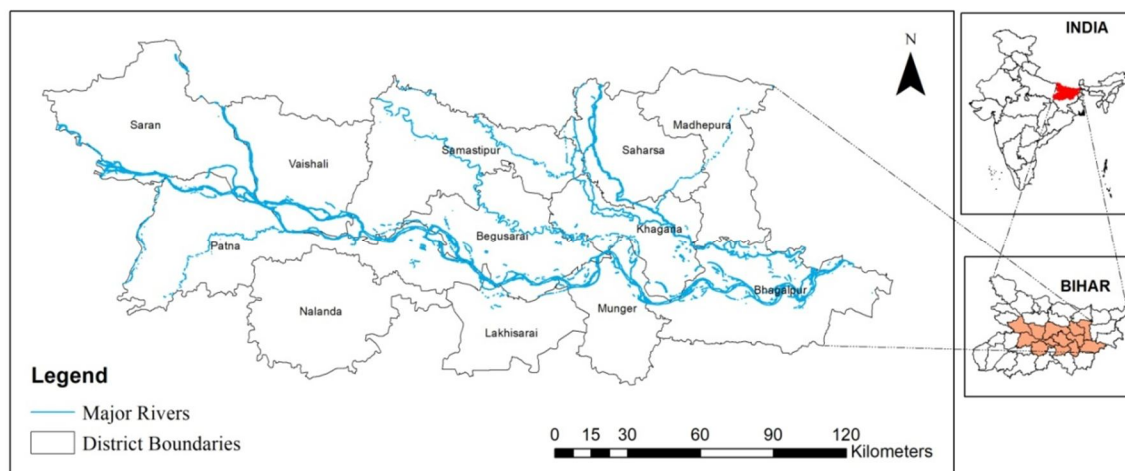


Figure 1: Study area map

B. Dataset Used

The satellite data used to perform this work is the Sentinel- 2 Level 2A products, which is georeferenced to WGS 84/ UTM projection zone. It's already atmospherically, geometrically ortho - rectified tile with $100 \times 100 \text{ km}^2$. The Sentinel 2 L2A satellite produces optical images of 16 bit unsigned integer using 13 multispectral bands from the electromagnetic spectrum with three different spatial resolutions of 10m, 20m and 60m. However, Bands 2, 3, 4 and 8 i.e. Blue, Green, Red and NIR in that order consist of 10m resolution while Bands 11, 12 (SWIR), 5, 6, 7, 8A are available in 20m resolution. To carry out the task of calculating water indexes, 20m resolutions dataset were used but due to the NIR having 10m and SWIR bands having 20m spatial resolutions (**Table 1**), upscaling of NIR band is done to 20m. This would eventually decrease the spatial information. The scenes for both pre and during flood time period was downloaded from ESA Copernicus hub (<https://scihub.copernicus.eu/>). For pre flood period, March, April and May 2019 data is used while for during flood period; imageries from the month of October 2019 were used.

Table 1: Bands and Spatial resolutions of Sentinel 2

Band	Spatial Resolution	Wavelength (nm)
B1	60	443
B2	10	490
B3	10	560
B4	10	665
B5	20	705
B6	20	740
B7	20	783
B8	10	842
B8A	20	865
B9	60	945
B10	60	1375
B11	20	1610
B12	20	2190

C. Precipitation Data

For the measurement of precipitation, daily average data for 5 months during the inundation period are generated from Tropical Rainfall Measuring Mission (TRMM) which provides best data for the region from 50° to 50° S with a spatial resolution of 0.25° x 0.25° was downloaded from Goddard Earth Sciences Data and Information Services Center (<https://disc.gsfc.nasa.gov>). The data is then processed to create monthly average rainfall maps.

III. METHODOLOGY

A. Spectral indexes

For this purpose, the water indexes were calculated using the temporal data of Sentinel 2B L2A data that was obtained from the ESA Copernicus. Calculation of the spectral index – Normalized Difference Water Index (NDWI) and Modified Normalized Difference Water Index (MNDWI) was a major task in this study. The Sentinel 2 satellite provides data in different spatial resolution of 10m and 20m, thus bands were resampled to similar resolution of 20m to access all the calculations. Top Of Atmosphere reflectance bands being more appropriate are to be used. The imagerys from Sentinel's Level 2A are already atmospherically corrected and so there's no further need to undergo pre processing (**Figure 2**).

1) NDWI

Normalized Difference Water Index (NDWI) helps to examine the water bodies using the Green and Near Infrared (NIR) bands from the electromagnetic spectrum. The formula was developed by McFeeters (1996). It is calculated as:

$$\text{NDWI} = (\text{GREEN} - \text{NIR}) / (\text{GREEN} + \text{NIR})$$

For Sentinel 2 data, NDWI = (B03 - B08) / (B03 + B08).

2) MNDWI

Xu (2006) modified the NDWI formula (as Modified Normalized Difference Water Index) replacing the NIR band to Shortwave Infrared (SWIR) band as he observed that more than NIR band the water bodies strongly absorbs in SWIR band. Xu's formula is calculated as:

$$\text{MNDWI} = (\text{GREEN} - \text{SWIR}) / (\text{GREEN} + \text{SWIR})$$

Sentinel 2 has two SWIR bands i.e. Band 11 and 12. Both the bands were used separately to perform the calculations.

$$\text{MNDWI 1} = (\text{B03} - \text{B11}) / (\text{B03} + \text{B11})$$

$$\text{MNDWI 2} = (\text{B03} - \text{B12}) / (\text{B03} + \text{B12})$$

B. Accuracy Assessment

For accuracy of the produced maps that were created using different spectral indexes, been evaluated. For examining performances of the resulted water bodies' maps, threshold values were used to detect the inundated areas. Using Google Earth, the reference data for accuracy assessment was obtained using validation points generated over the imagery and separate the water and non – water region. On the basis of the Overall Accuracy and Kappa, Optimum threshold were chosen. The worse thresholds were eliminated using visual interpretation and then an optimum threshold is selected. And finally with highest kappa result, flood maps were created.

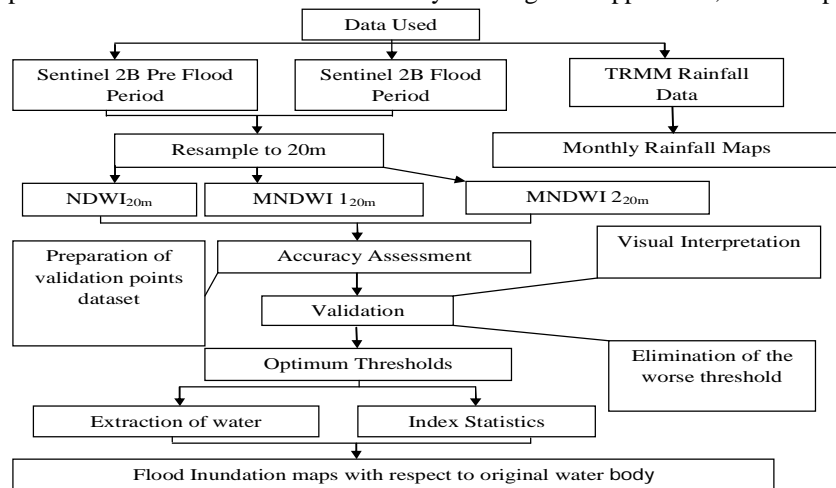


Figure 2: Methodology Chart

IV. RESULTS AND DISCUSSIONS

A. Comparison Between Different Water Indexes

Figure 3 represents the water indexes for both pre and during flood. It is observed that MNDWI 1_{20m} had dissimilarity in the highest values obtained for both Scenes of pre and during flood period. In both MNDWI 1_{20m} and MNDWI 2_{20m} indexes spatial details of water bodies were represented more clearly by resulting greater values for the during flood period.

During the pre time the NDWI $_{20m}$ index for Scene A evaluated a lowest value of -0.74 and a highest of 0.42. While for Scene B, NDWI $_{20m}$ ranged between -0.58 to 0.70. MNDWI 1_{20m} index for Scene A resulted -0.74 as the highest of 0.63 and lowest of -0.55. The lowest values for all the indexes in Scene B were similar. MNDWI 2_{20m} for Scene B resulted highest with 0.75.

For the during flood period it was observed that Scene A NDWI $_{20m}$ yield between -0.76 to 0.73. MNDWI 1_{20m} showed results from -0.60 to 0.96. MNDWI 2_{20m} has values between -0.57 to 0.99. For Scene B, NDWI $_{20m}$ ranged from -0.84 to 0.79. MNDWI 1_{20m} resulted between -0.69 to 0.98. While MNDWI 2_{20m} for Scene B resulted between -0.69 to 0.98.

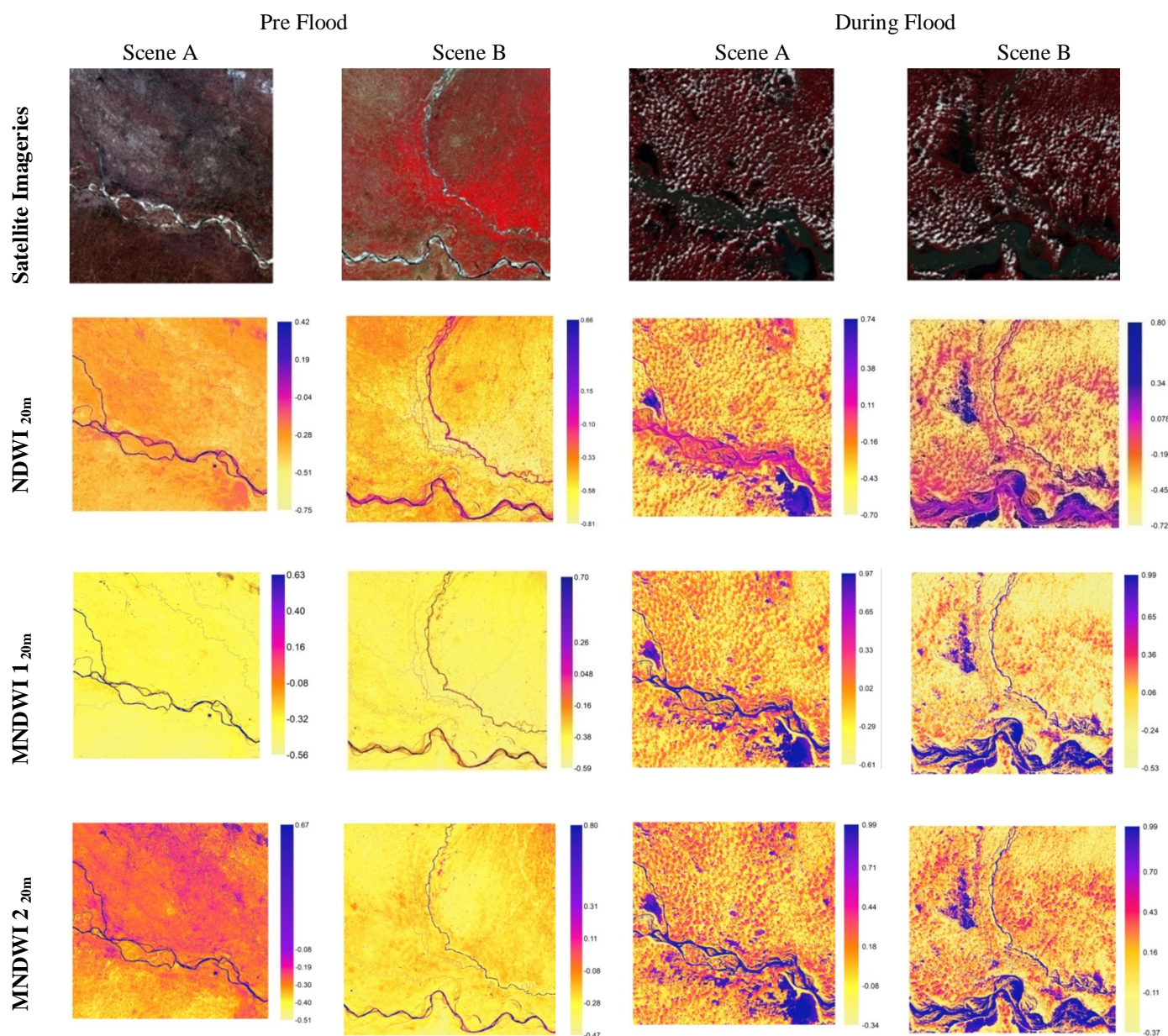
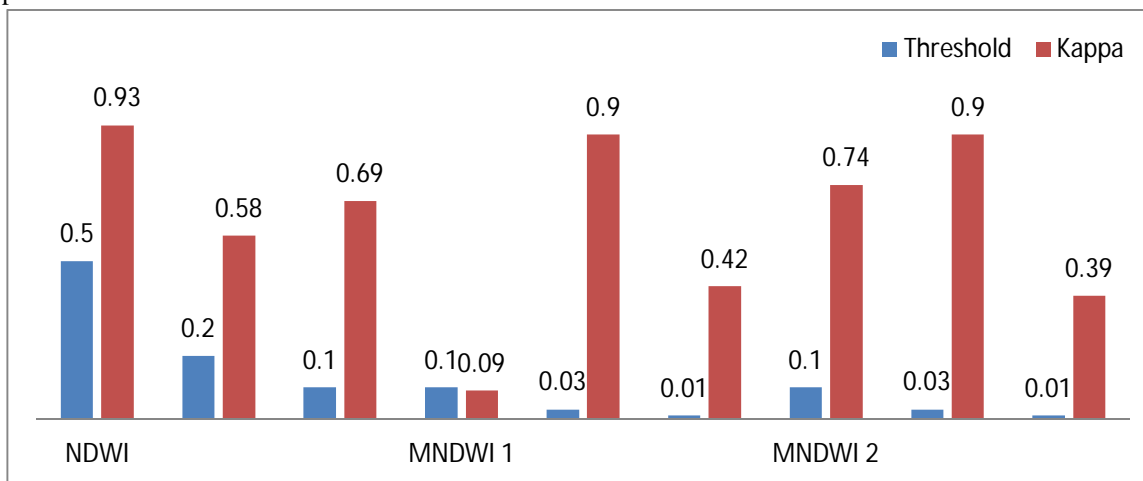


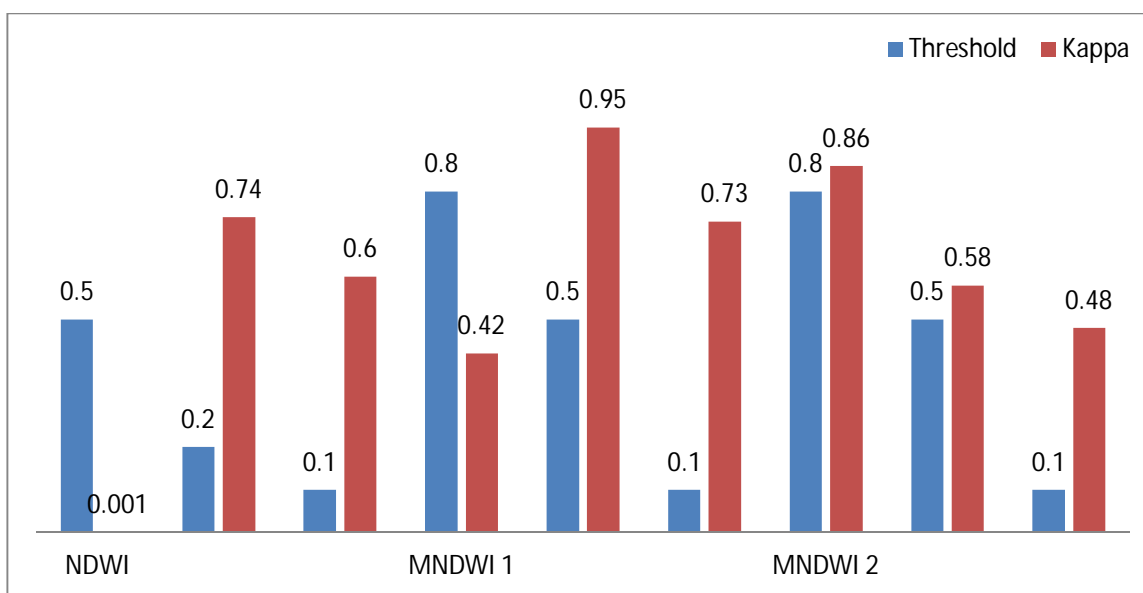
Figure 3: Comparison between the water indexes – pre and during flood period

B. Accuracy Assessment

Table 2 represents the performance of all the water indexes for the extraction of flood water. It is assessed for the entire study area and a comparison has been conducted to evaluate the performance by each of the methods. Using the three proposed methods, the results for delineating water bodies was showed highest OA by NDWI_{20m} of 0.93 in pre flood period and for MNDWI 1_{20m} it resulted to be 0.91 for the during flood period. MNDWI 2_{20m} shows the lowest OA in both the scenario. While it is observed that for the highest OA also has the highest Kappa of 0.96 in NDWI_{20m} and 0.95 in MNDWI 1_{20m} for the two periods. The OA was increased in the flood time with a maximum of 0.91 along with the Kappa of 0.95 that was resulted by MNDWI 1_{20m}. Figure 4 shows the graphical representation of the assessment.



(a)



(b)

Figure 4: Accuracy Assessment of water index for pre (a) and during (b) flood period

It is observed that for all the thresholds in both pre and during flood scenario (**Table 2**) PA is higher in most of the indexes. Simultaneously, the lower UA is evident that non water surfaces were misclassified to be water. In order to lessen the misclassification an optimum threshold (**Table 2**) has to be established that can represent the actual flood inundation on the surface. For this the binary imagery is carried forward with the trial and error method with the index maps as validation data. The optimum threshold with highest OA and Kappa is selected thereafter to determine the inundated areas for both pre and during flood event. Using the water indexes index maps was derived each for pre and during flood scenario.

C. Comparison Between Resulting Water Bodies' Maps

The **Figure 5** represents a comparison of water bodies for the pre and during flood moment. In **Scene A**, the $NDWI_{20m}$ omitted some linear features. $MNDWI_{20m}$ in **Scene B** misclassified some areas as water. For the during flood event the $NDWI_{20m}$ index resulted a large amount of isolated pixels are mapped particularly in the **Scenes B**. This might be due to the existence of clouds in the imagery which merged with the water pixels. For **Scene A**, it is also observed that the $NDWI_{20m}$ index have more water logging part and the water body maps created by both the $MNDWI_{20m}$ precisely removed the isolated pixels that were susceptible of clouds. $MNDWI_{20m}$ had eliminated some details of the water logging patches **Scene A**. The streams are also not visible as compared to the other indexes and there was lack in detailed mapping for the water bodies which resulted as jagged in many areas. $MNDWI_{120m}$ having less misclassification has given more precise outcome as in comparison with the two other methods.

Table 2: Accuracy Assessment for the different indexes of all the four scenes for pre and during flood period

	Water Index	$NDWI_{20m}$			$MNDWI_{120m}$			$MNDWI_{20m}$		
	Threshold	0.5	0.2	0.1	0.1	0.03	0.01	0.1	0.03	0.01
PRE FLOOD	PA	1	0.46	1	0.18	1	1	0.6	1	0.8
	UA	0.93	1	0.62	1	0.21	0.3	1	0.14	0.13
	OA	0.96	0.73	0.81	0.65	0.60	0.59	0.88	0.57	0.56
	Kappa	0.93	0.58	0.69	0.09	0.9	0.42	0.74	0.9	0.39
	Threshold	0.5	0.2	0.1	0.8	0.5	0.1	0.8	0.5	0.1
DURING FLOOD	PA	0.97	1	1	0.42	1	0.73	0.71	0.77	0.73
	UA	0.97	0.39	0.61	0.63	0.92	0.87	0.59	0.7	0.85
	OA	0.94	0.89	0.86	0.71	0.91	0.88	0.79	0.94	0.72
	Kappa	0.001	0.74	0.6	0.42	0.95	0.73	0.86	0.58	0.48
	Threshold	0.5	0.2	0.1	0.8	0.5	0.1	0.8	0.5	0.1

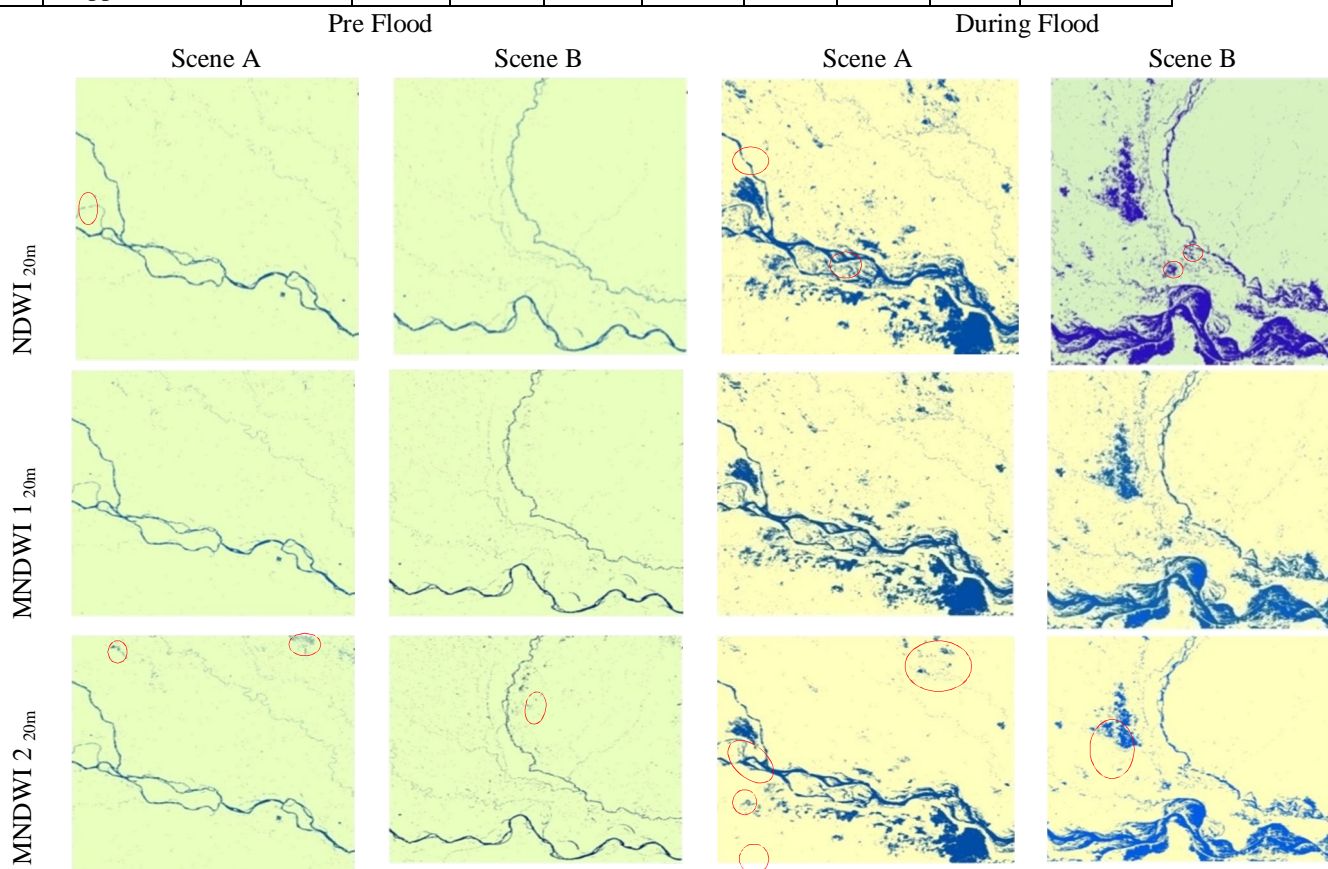


Figure 5: Comparison of spectral water indexes using optimum thresholds for pre and during flood period

D. Statistical Calculations

Table 3 represents the optimum threshold values evaluated from both before and after flood scenario to detect water. For the during time scene, higher thresholds resulted better classification of flood water by MNDWIs but lower threshold values is proved to detect water more accurately by NDWI. The optimum threshold of NDWI is 0.5 and 0.2 for pre flood and during flood respectively. While for MNDWIs it is 0.03 for pre flood situation and for during flood time it's 0.5 for MNDWI 1 and 0.8 for MNDWI 2 respectively.

The estimation results of $NDWI_{20m}$, $MNDWI_{120m}$ and $MNDWI_{220m}$ values in the water bodies' samples as yield by the indexes in the pre and during flood event with the changes in the values are displayed in **Table 4**.

Table 3: Optimum Thresholds

Period	Optimum Threshold	
Water Index	Pre Flood	During Flood
$NDWI_{20m}$	0.5	0.2
$MNDWI_{120m}$	0.03	0.5
$MNDWI_{220m}$	0.03	0.8

For the pre flood time the minimum values of water bodies were -0.3 for $MNDWI_{120m}$ and -0.4 for $MNDWI_{220m}$ while for $NDWI_{20m}$ the minimum values were -0.6. $MNDWI_{20m}$ has the higher maximum and minimum values as compared to $NDWI_{20m}$. There is increase in $MNDWI_{220m}$ mean value of 0.40 than that of $NDWI_{20m}$ which has 0.26. $MNDWI_{220m}$ has the highest SD of 0.7 while $NDWI_{20m}$ has the lowest of 0.14 in the water bodies for the pre flood period.

For the during flood event the threshold values for water bodies resulted from -0.6 to 0.9 for $NDWI_{20m}$ and for $MNDWI_{120m}$ min value for the water bodies area -0.4 and it ranged up to 1. While for $MNDWI_{220m}$ it yields between -1 to 1. $MNDWI_{220m}$ yields the lowest SD of 0.07 while it shows the highest mean of 0.9 for the during flood period.

Table 4: Statistics in water bodies for pre and during flood period

Period	Pre Flood			During Flood		
Water Indexes	$NDWI_{20m}$	$MNDWI_{120m}$	$MNDWI_{220m}$	$NDWI_{20m}$	$MNDWI_{120m}$	$MNDWI_{220m}$
Statistics						
Min	-0.6035	-0.3842	-0.4106	-0.6955	-0.4920	-1.0000
Max	0.7073	1.0000	0.9981	0.9968	1.0000	1.0000
Mean	0.2628	0.3779	0.4039	0.3511	0.8065	0.9019
SD	0.1476	0.1556	0.1711	0.1698	0.1427	0.0730

E. Meterological Observations

The graphical representation of average precipitation of the entire study region during the months of June to October, 2019 is shown in Figure 6. The monthly average rainfall is witnessed to vary from 521mm to 142mm. Throughout monsoon 2019, rainfall was 263mm, 521mm, 243mm, 405mm and 142mm during June, July, August, September and October respectively. The highest rainfall was received in the month of July. From the monthly distribution rainfall maps (Figure 7), it is evident that the districts of Khagaria, Bhagalpur and Begusrai received heaviest rain throughout the 2019 monsoon season. Khagaria and Bhagalpur received more than 650mm rainfall in July while Patna and Saran receives highest rainfall more than 600mm during September which is more than the monthly average.

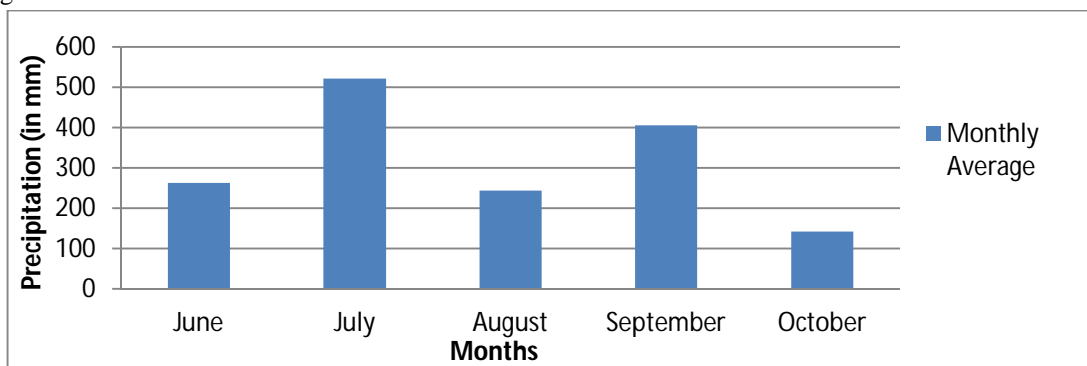


Fig 6: Monthly average precipitation during inundation period

Figure 6: Monthly average graphica plot of TRMM precipitation data 2019

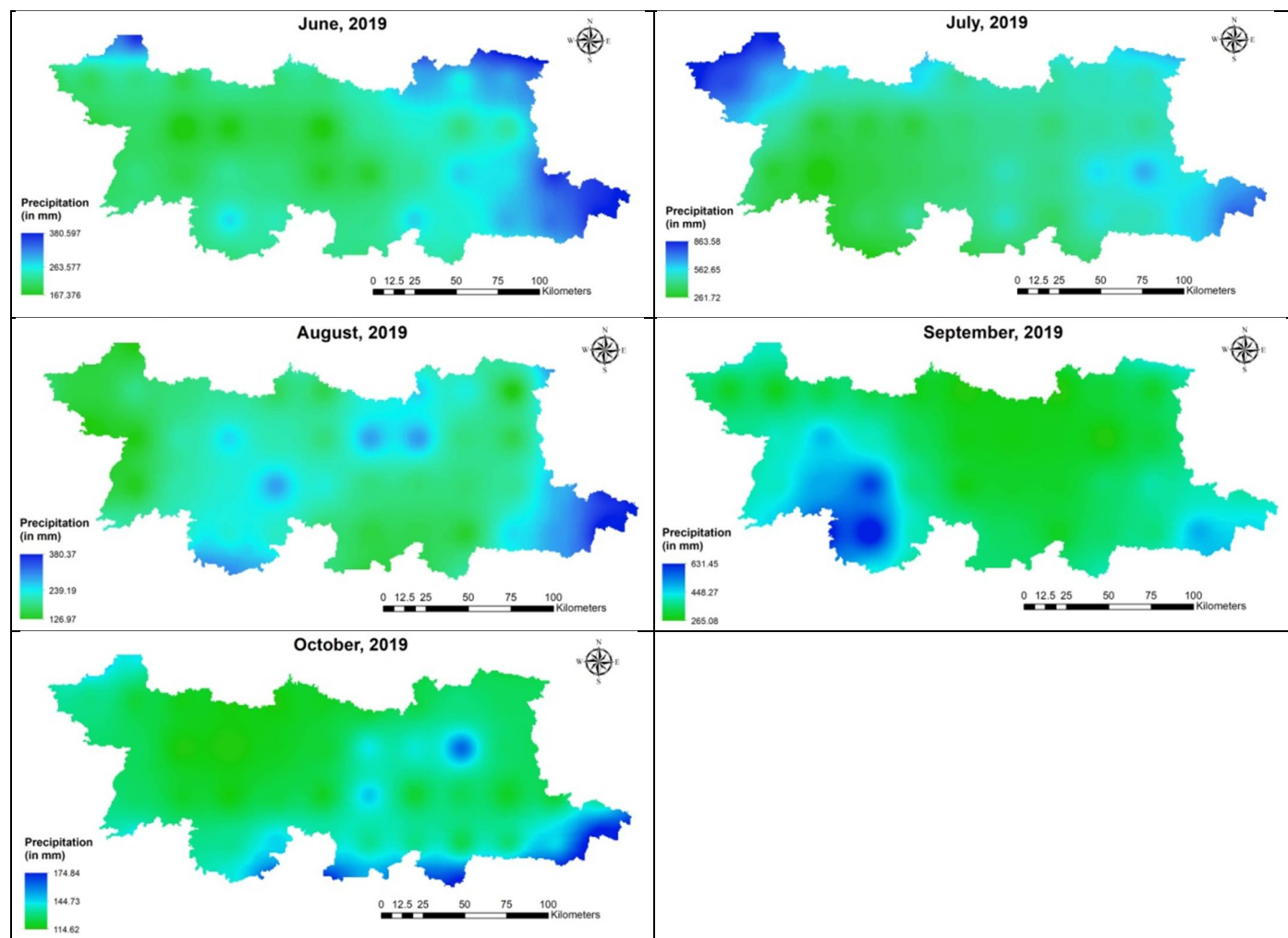


Figure 7: Rainfall Distribution Maps of June to October, 2019

F. Inundated Areas

Figure 8 shows the areas of Central Bihar along the Ganga River was severely affected by flood in 2019. The most flood affected areas of 2019 are the districts of Patna, Begusrai, Saran, Samastipur, Khagaria, Bhagalpur, Munger. About 50% of Patna district was flood until month of October. The areas of eastern Samastipur ads Saran district lying along the tributaries of Ganga were also highly flooded. However Khagaria, Bhagalpur and Begusrai experiencing the highest rainfall remained flooded mostly in its southern parts near the bank of Ganga River.

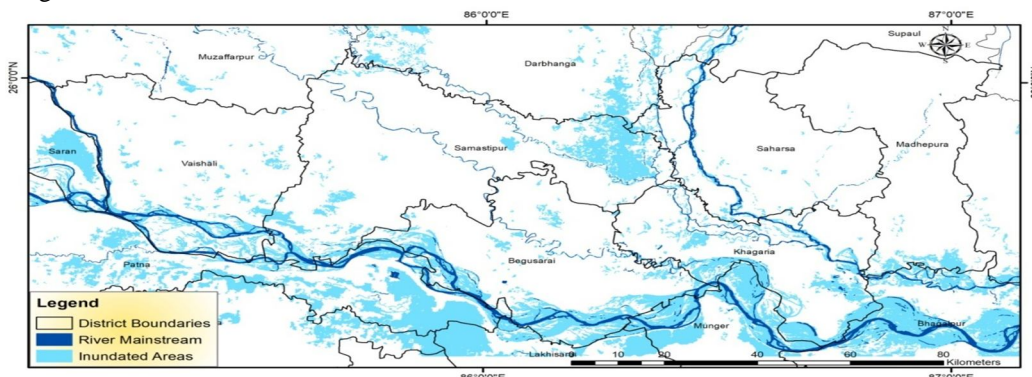


Figure 8: Flood Inundated Areas of Central Bihar Districts for 2019

V. CONCLUSION

The present study is based on extraction of flood inundation from the space borne technology of Sentinel 2 mission which has suitably been able to capture the devastated flood disaster along the Ganga River of Bihar region during 2019. The spectral indexes methods of NDWI and MNDWI were calculated which helped to delineate the inundated areas. The SWIR and Green bands provided by Sentinel – 2 have spatial resolutions of 10m and 20m respectively. And to calculate the water indexes, spatial resolution was upscaled to 20m. The spectral indexes i.e. NDWI, MNDWI 1 and MNDWI 2 have played significant role to delineate flooded areas in the region.

One of the tricky tasks in this study was the selection of optimum threshold and evaluation of the spectral indexes. The threshold values played a vital role to precisely detect the inundated areas. It differed in every index for both pre and during flood occurrence. The lower threshold values for the pre flood time for MNDWIs gave more accurate results then the higher ones while this was the opposite for the during flood event. NDWI yield optimum results with lower threshold in during flood scenario.

These methods are used to extract water and separate them from the non water surface on the basis of threshold values. For the during time scene, higher thresholds resulted better classification of flood water by MNDWIs but lower threshold values is proved to detect water more accurately by NDWI. The highest Kappa of 0.95 and Overall Accuracy (OA) of 0.91 for during the flood event is produced by MNDWI 1 and for the pre flood time NDWI resulted the highest Kappa of 0.93.

For the imageries in the pre inundation period, some linear features were omitted by NDWI and pixels were misclassified by MNDWI 1_{20m}. Whereas for the during flood data, presence of clouds was an obstacle for the reason that the pixels got merged and this became the reason of misclassification as water. Most of the misclassification was yield by NDWI_{20m}. MNDWI 2_{20m} lacked in detailed mapping eliminating some pixels which affected its accuracy. Overall in the present study, MNDWI 1_{20m} have less misclassification and yield better results into comparison with the two other methods. MNDWI 1_{20m} specifically removed misclassified and isolated pixels classified as water. The research in the particular region of Sentinel 2 data proved that MNDWI 1 is the more capable of delineating flood water more precisely. The study also demonstrates that this method can be applicable to indentify water bodies in both perennial and non perennial period.

VI. ACKNOWLEDGEMENT

Authors are thankful to Indian Institute of Remote Sensing (IIRS), Dehradun for providing the lab facility to complete the study. First author is grateful to IIRS, Dehradun for giving her permission to undertake Masters' Degree Dissertation at the Institute. Widespread support provided by the Remote Sensing and GIS Department, Kumaun University, SSJ Campus, Almora is also acknowledged.

REFERENCES

- [1] Acharya, Tri Dev, Anoj Subedi, and Dong Ha Lee. "Evaluation of water indices for surface water extraction in a Landsat 8 scene of Nepal." *Sensors* 18, no. 8 (2018): 2580.
- [2] Bhatt, C. M., Rao, G. S., Manjushree, P., & Bhanumurthy, V. (2010). Space based disaster management of 2008 Kosi floods, North Bihar, India. *Journal of the Indian Society of Remote Sensing*, 38(1), 99-108.
- [3] DMSG, 2001: The Use of Earth Observing Satellites for Hazard Support: Assessments & Scenarios. Committee on Earth Observation Satellites Disaster Management Support Group, Final Report, NOAA, Dept. Commerce, USA.
- [4] Du, Yun, Yihang Zhang, Feng Ling, Qunming Wang, Wenbo Li, and Xiaodong Li. "Water bodies' mapping from Sentinel-2 imagery with modified normalized difference water index at 10-m spatial resolution produced by sharpening the SWIR band." *Remote Sensing* 8, no. 4 (2016): 354.
- [5] Goodell, C., & Warren, C. (2006). Flood inundation mapping using HEC-RAS. *Obras y Proyectos*, (2), 18-23.
- [6] Ho, L. T. K., Umitsu, M., & Yamaguchi, Y. (2010). Flood hazard mapping by satellite images and SRTM DEM in the Vu Gia–Thu Bon alluvial plain, Central Vietnam. *International archives of the photogrammetry, remote sensing and spatial information science*, 38(Part 8), 275-280.
- [7] McFeeters, Stuart K. "Using the normalized difference water index (NDWI) within a geographic information system to detect swimming pools for mosquito abatement: A practical approach." *Remote Sensing* 5, no. 7 (2013): 3544-3561.
- [8] National Geographic. Floods. Available online: <https://www.nationalgeographic.com/environment/natural-disasters/floods/> (accessed on 15 April 2018).
- [9] Rai, Praveen Kumar, and Kshitij Mohan. "Remote Sensing data & GIS for flood risk zonation mapping in Varanasi District, India/Utilizarea SIG siteledetectieipentru cartarea zonelor de risc la inundatii in districtul Varanasi, India." In *Forum Geografic*, vol. 13, no. 1, p. 25. University of Craiova, Department of Geography, 2014.
- [10] Rastogi, A. K., P. K. Thakur, G. Srinivasa Rao, S. P. Aggarwal, V. K. Dadhwal, and P. Chauhan. "Integrated Flood Study of Bagmati River Basin with Hydro Processing, Flood Inundation Mapping & 1-D Hydrodynamic Modeling Using Remote Sensing and GIS." *ISPRS Annals of the Photogrammetry, Remote Sensing and Spatial Information Sciences* 4 (2018): 165-172.
- [11] Xu, Hanqiu. "Modification of normalised difference water index (NDWI) to enhance open water features in remotely sensed imagery." *International journal of remote sensing* 27, no. 14 (2006): 3025-3033.



10.22214/IJRASET



45.98



IMPACT FACTOR:
7.129



IMPACT FACTOR:
7.429



INTERNATIONAL JOURNAL FOR RESEARCH

IN APPLIED SCIENCE & ENGINEERING TECHNOLOGY

Call : 08813907089  (24*7 Support on Whatsapp)